sustainability

MDPI

Article

Effects after 1500 Hardening Days on the Microstructure and Durability-Related Parameters of Mortars Produced by the Incorporation of Waste Glass Powder as a Clinker Replacement

Rosa María Tremiño [1], Teresa Real-Herraiz [2], Viviana Letelier [3], Fernando G. Branco [4] and José Marcos Ortega [1,*]

[1] Departamento de Ingeniería Civil, Universidad de Alicante, Ap. Correos 99, 03080 Alicante, Spain; rmta2@alu.ua.es
[2] Instituto de Matemática Multidisciplinar, Universidad Politécnica de Valencia, Camino de Vera s/n, 46022 Valencia, Spain; tereaher@upv.es
[3] Departamento de Obras Civiles, Universidad de la Frontera, Av. Fco. Salazar, Temuco 01145, Chile; viviana.letelier@ufrontera.cl
[4] ISISE, Department of Civil Engineering, University of Coimbra, R. Luís Reis Santos, 3030-788 Coimbra, Portugal; fjbranco@dec.uc.pt
* Correspondence: jm.ortega@ua.es; Tel.: +34-96-5903-400 (ext. 2470)

Abstract: One of the ways of lessening the CO_2 emissions of cement industry consists of replacing clinkers with supplementary cementitious materials. The required service life of real construction elements is long, so it is useful to characterize the performance of these materials in the very long term. Here, the influence of incorporating waste glass powder as a supplementary cementitious material, regarding the microstructure and durability of mortars after 1500 hardening days (approximately 4 years), compared with reference mortars without additions, was studied. The percentages of clinker replacement by glass powder were 10% and 20%. The microstructure was studied using impedance spectroscopy and mercury intrusion porosimetry. Differential thermal and X-ray diffraction analyses were performed for assessing the pozzolanic activity of glass powder at the end of the time period studied. Water absorption after immersion, the steady-state diffusion coefficient, and length change were also determined. In view of the results obtained, the microstructure of mortars that incorporated waste glass powder was more refined compared with the reference specimens. The global solid fraction and pores volume were very similar for all of the studied series. The addition of waste glass powder reduced the chloride diffusion coefficient of the mortars, without worsening their behaviour regarding water absorption after immersion.

Keywords: waste glass powder; supplementary cementitious materials; very long-term; sustainability; microstructure; durability

Citation: Tremiño, R.M.; Real-Herraiz, T.; Letelier, V.; Branco, F.G.; Ortega, J.M. Effects after 1500 Hardening Days on the Microstructure and Durability-Related Parameters of Mortars Produced by the Incorporation of Waste Glass Powder as a Clinker Replacement. *Sustainability* **2021**, *13*, 3979. https://doi.org/10.3390/su13073979

Academic Editor: Antonio Caggiano

Received: 21 February 2021
Accepted: 29 March 2021
Published: 2 April 2021

1. Introduction

The reduction of CO_2 emissions of the most pollutant industrial sectors is an important topic of study [1,2]. In this regard, the construction sector in general, and particularly the cement industry, are developing several strategies in order to increase their contribution to sustainability, in line with the current worldwide goals focused on reducing global warming. Among these strategies, the search for eco-friendly materials has experienced great progress in the last years [3,4].

In relation to cement-based materials, one of the ways of lessening the CO_2 emissions produced by their production consists of partially or totally replacing the clinker by additions such as supplementary cementitious materials [5]. There are several classical additions [6,7] that have been used for decades, such as ground granulated blast-furnace slag, fly ash, and silica fume. Most of them are waste coming from other industrial pro-

cesses, so their use also has other environmental advantages, such as avoiding their storage in landfills.

However, the availability of these classical additions could be reduced in the future, especially in the case of fly ash, because of the progressive closing or transformation of coal-fired power stations, as well as in relation to the current context focused on lessening pollution. Therefore, the research of new supplementary cementitious materials still continues at present. For examples of these new additions, it is interesting to highlight rice husk ash [8], brick powder [9], and red mud [10], among others.

Regarding glass waste, their quantity has progressively risen in recent years, because of the increased use of glass products [11], now representing approximately 5% of home residues [12]. The percentage of glass recycling varies depending on the country, reaching high recycling rates in the European Union [13], while in America, they are still low, with the particular case of USA with, for example, only 34% of glass waste being recycled in 2014 [12].

Among the different ways for reusing this waste and reducing its environmental impact, its possible utilization as an addition in cement-based materials has been reported by several researchers [14–17], because of its high silica content [16–18], which would allow for the development of pozzolanic properties [14–17]. In addition, it has been pointed out that recycled glass powder has the potential for improving the physical and mechanical properties of mortars [19] and for reducing the heat of hydration [20], at least in the short term. It has also been reported that mixtures containing glass powder perform satisfactorily with respect to drying shrinkage, alkali reactivity, and chloride ion penetrability in the short term [21], producing reductions in pore size and connectivity [22]. Other work [23] has shown that the results of using a Portuguese recycled glass material as an aggregate or pozzolan in cement-based mortars can decrease the alkali silica reaction effects, and its efficiency is related with the replacement ratio.

Several studies [24,25] have analyzed the combination of glass powder with other additions such as rice husk ash and metakaolin after a short time, observing a good performance of this addition. Regarding the behavior of cementitious materials in outdoor environments, it has been pointed out [26] an improvement in resistance to chloride ion penetration without reducing the mechanical performance after 100 exposure days. However, some studies [15,16,20,27,28] have reported a delay in the development of properties in cement-based materials that incorporated glass powder compared withcontrol binders.

As has been indicated previously, it is important to highlight that the majority of existing research has analysed the effect of volcanic powder at relatively short hardening ages [29,30]. Nevertheless, the required service life of real construction elements, which belong to buildings, structures, and other engineering works, is usually long [31]. Thus, for assessing if the new supplementary cementitious materials, such as waste glass powder, are adequate for being used in these real construction elements, it is necessary to characterize their performance in the very long term, after hardening periods of several years.

Therefore, the main objective of this research is to get information about the influence of the incorporation of waste glass powder as a supplementary cementitious material on the microstructure and durability of mortars after approximately 4 hardening years (1500 days), compared with reference mortars without additions. The percentages of clinker replacement using glass powder were 10% and 20%. The pore network of the mortars was studied using the non-destructive impedance spectroscopy technique and mercury intrusion porosimetry. In order to assess the pozzolanic activity development of the glass powder at the end of the studied time period, differential thermal and X-ray diffraction analyses were performed. Regarding the durability-related parameters, the water absorption after immersion and the steady-state diffusion coefficient obtained from the saturated samples' resistivity were determined. Finally, the length change of the mortars was measured after 1500 hardening days for evaluating if the glass powder produced any effect in this regard.

2. Materials and Methods

2.1. Materials and Sample Preparation

In this work, mortars that incorporated the addition of waste glass powder (GP) were studied. The waste glass came from recycling containers and the glass powder was obtained through a process of crushing and dry grinding the original residues. The chemical composition of the glass powder is shown in Table 1 and its particle size distribution is represented in Figure 1.

Table 1. Chemical properties of glass powder.

Composition	Value
Al_2O_3	2.90%
SiO_2	64.32%
Na_2O	13.03%
CaO	18.18%
Fe_2O_3	-
K_2O	1.56%
SO_3	-
MgO	-

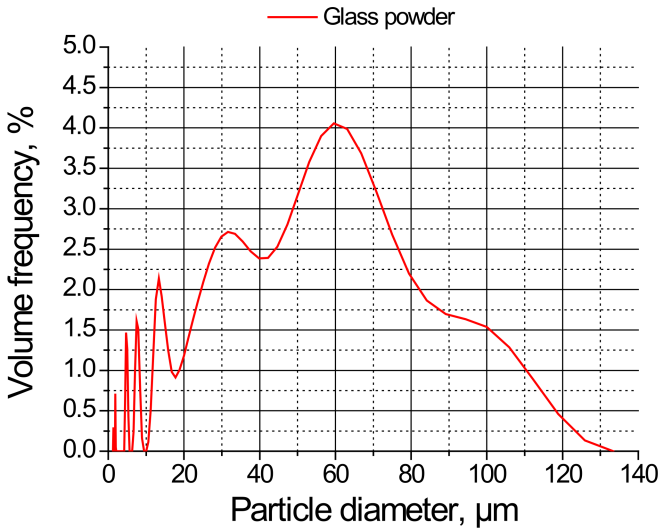

Figure 1. Particle size distribution of glass powder.

The mortars were made with binders that combined glass powder and a commercial ordinary Portland cement CEM I 42.5 R [32]. First, the reference mortars without glass powder were prepared, designated as REF in the results and discussion sections. Then, two series of mortars with GP additions were also made, incorporating 10% and 20% in weight as a replacement of the abovementioned cement CEM I 42.5 R. These series were designed as GP10 and GP20, respectively. The water to cement ratio was 0.5 and the aggregate to cement ratio was 3:1 for all of the mortars. The fine aggregates accomplished the prescriptions of standard UNE-EN 196-1 [33].

The prepared samples were cured during the first 24 h, and were stored in a chamber at 20 °C with 95% relative humidity (RH). Two types of specimens were prepared. On one hand, cylindrical specimens with 10 cm diameter and 15 cm height were made. Once de-molded, these specimens were cut to obtain disks with a 1 cm thickness, which were used for the impedance spectroscopy technique measurements and for the determination of the steady-state diffusion coefficient, in order to obtain pieces for the mercury intrusion porosimetry test and for the determination of the water absorption by immersion, as well as for getting powder for the differential thermal analyses. On the other hand, prismatic samples with dimensions of 25 mm × 25 mm × 285 mm were also prepared, which were

used for the length change measurements. Finally, all of the samples were kept in optimum laboratory conditions (20 °C and 100% RH) for 1500 hardening days (approximately 4 years), after which they were tested.

2.2. Mercury Intrusion Porosimetry

The mercury intrusion porosimetry technique allows for obtaining information about the microstructure of materials [34,35]. In this work, this test was performed using a porosimeter Poremaster-60 GT model manufactured by Quantachrome Instruments (Boynton Beach, FL, USA). Before the test, the specimens were dried in an oven at 50 °C for 48 h. The results analyzed in this work were the total porosity, pore size distribution, and percentage of Hg retained at the end of the experiment. Two measurements were made on each type of mortar at the hardening age studied.

2.3. Impedance Spectroscopy

Regarding the impedance spectroscopy, recently, it was successfully used for getting information about the microstructure of different types of cement-based materials [36–38]. Here, the impedance spectroscopy measurements were performed using an Agilent 4294A analyzer (Agilent Technologies, Kobe, Japan). This device takes capacitance measurements ranging between 10^{-14} F and 0.1 F, with a maximum resolution of 10^{-15} F. Circular electrodes with an 8 cm diameter were used, consisting of flexible graphite attached to a piece of copper with the same diameter, in order to obtain the impedance spectra. The frequencies ranged between 100 Hz and 100 MHz.

Contacting and non-contacting measurement methods were used [36]. The experimental data were fit to the equivalent circuits proposed by Cabeza et al. [36]. Those circuits consisted of several resistances and capacitances [36] (see Figure 2). The R_1 resistance provides data about the percolating pores in the sample [36], the R_2 resistance provides information about the pores in general [36], the C_1 capacitance provides information about the solid fraction of the sample [36], and the C_2 capacitance is associated with the surface of the pores in contact with the electrolyte that fills the pore network of the material [37]. Here, because of their greater accuracy, only the values of parameters R_2, C_1, and C_2 with the non-contacting method were analyzed. The values of the R_1 resistance, which could only be obtained using the contacting method, were only used for obtaining the steady-state chloride diffusion coefficient. Eight different disks were analyzed with this technique for each mortar type.

Figure 2. (**a**) Equivalent circuit used for fitting the impedance spectra obtained using the contacting method. (**b**) Equivalent circuit used for fitting the impedance spectra obtained using the non-contacting method.

2.4. Differential Thermal Analysis

The differential thermal analyses were performed using a simultaneous TG-DTA model TGA/SDTA851e/SF/1100 from Mettler Toledo, which allows for working from room temperature to 1100 °C. The chosen heating ramp was 20 °C/min up to 1000 °C in an N_2 atmosphere. The curve weight derivate versus temperature was determined for each mortar type.

2.5. X-Ray Diffraction (XRD)

X-ray diffractions were performed using a Bruker D8 Advance diffractometer (Bruker Española S.A., Madrid, Spain). The spectrum was registered with stepping intervals from 4° to 60° at 0.05° in the Θ- Θ mode (X-ray tube power: 40 kV and 40 mA). The X-ray spectra were obtained for each mortar type after 1500 hardening days.

2.6. Water Absorption

The absorption after immersion was determined following the procedure included in the ASTM Standard C642-06 [39]. Six pieces taken from disks of a 1-cm thickness were tested for each kind of mortar studied.

2.7. Steady-State Diffusion Coefficient

The steady-state chloride diffusion coefficient was obtained from the electrical resistivity of the saturated samples. The resistivity was calculated from the R_1 impedance spectroscopy values measured in the water saturated samples. As has been previously explained, the R_1 impedance resistance is related to the pores that cross the sample [36] and is therefore equivalent to the electrical resistance of the sample. For each mortar series, six different disks with a1 cm thickness were tested. Finally, the steady-state diffusion coefficient was calculated using the following expression [40]:

$$D_S = \frac{2 \times 10^{-10}}{\rho} \quad (1)$$

where D_s is the chloride steady-state diffusion coefficient through the sample (m^2/s) and ρ is the electrical resistivity of the specimen ($\Omega \cdot m$).

2.8. Length Change

In order to assess whether the addition of glass powder produced the development of the expansion or shrinkage phenomena, in the mortars with waste glass powder, compared with the reference ones, their length change in percentage was determined after 1500 hardening days. Once de-moulded, the initial length of the prismatic samples was measured using a length comparator according to ASTM Standard C596-01 [41]. This length was the starting point of reference. At the end of the studied period, their length was measured again with the same procedure. Finally, from both measurements, the percentage of length change with respect to the initial length after 1500 hardening days was calculated. For each mortar type, six prismatic specimens with dimensions of 25 mm × 25 mm × 285 mm were tested.

3. Results

3.1. Mercury Intrusion Porosimetry

The total porosity results obtained after 1500 days for the three mortar series analyzed are depicted in Figure 3. The values of this parameter were similar for the REF, GP10, and GP20 specimens, although it was slightly lower for the mortars that incorporated 10% of waste glass powder compared with the reference ones. The total porosity noted for the GP20 mortars was not much higher that that observed for the GP10 and REF series.

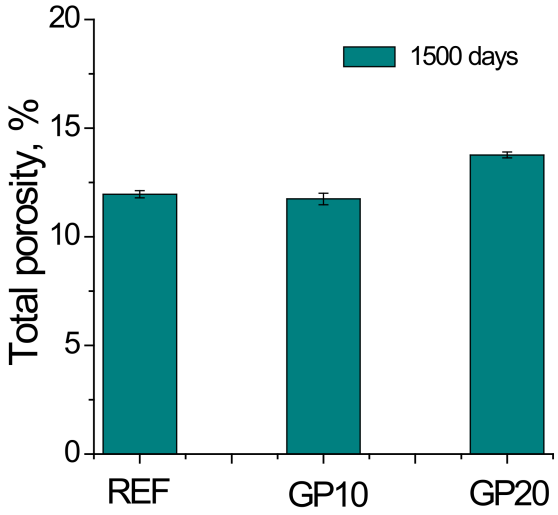

Figure 3. Total porosity results obtained for the studied mortar series. Error bars in this figure and in the following represent the standard deviation.

With respect to the pore size distributions of the studied mortars, they can be observed in Figure 4. The percentage of pores with smaller diameters was greater for the specimens with a glass powder addition in comparison with the reference ones, which was especially noticeable for pores with sizes lower than 10 nm. When comparing the pore size distributions of the GP10 and GP20 mortars, those with a greater content of glass powder presented a higher presence of finer pores. Therefore, according to these results, the addition of waste glass powder as a clinker replacement produced a greater refinement of the pore network of the mortars after 1500 hardening days.

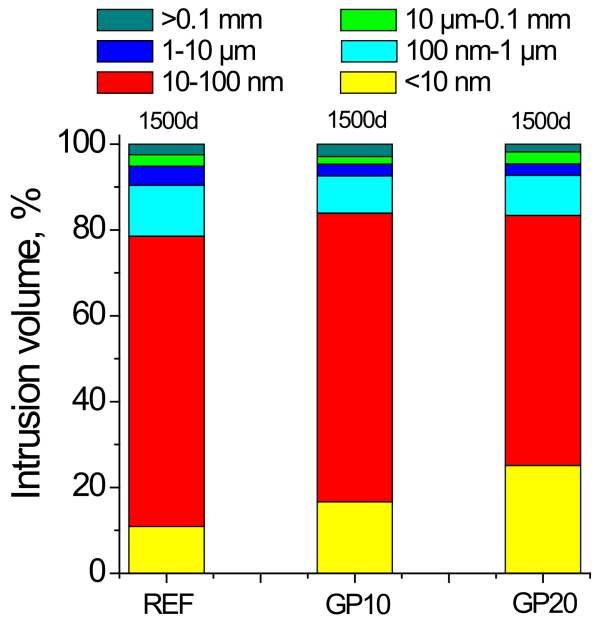

Figure 4. Pore size distributions noted for reference mortar without glass powder (REF), mortar with 10% glass powder (GP10), and mortar with 20% glass powder (GP20).

The results of mercury retained at the end of mercury intrusion porosimetry test are represented in Figure 5. This parameter was relatively similar for all of the mortars studied, although it was slightly higher for the specimens with glass powder, especially the GP10 ones.

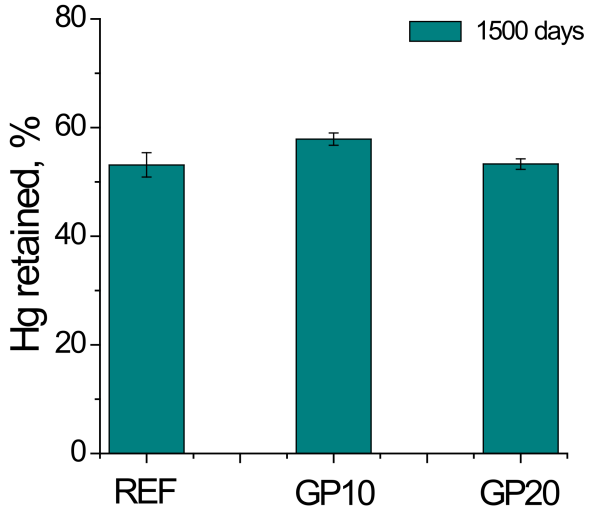

Figure 5. Results of percentage of mercury retained at the end of the mercury intrusion porosimetry test for the studied mortars after1500 hardening days.

3.2. Impedance Spectroscopy

Regarding the impedance capacitances, the results of capacitance C_1 are shown in Figure 6. This parameter was slightly higher as increased the glass powder content in the samples. However, scarce differences in this capacitance were observed overall between the different mortar series analyzed.

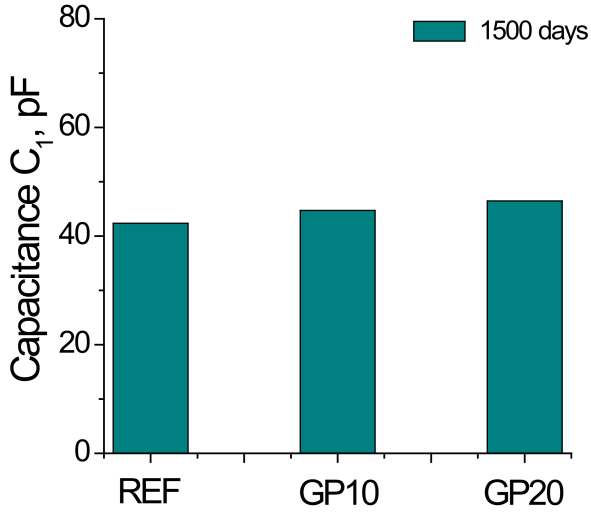

Figure 6. Results of capacitance C_1 for the analyzed mortars.

The capacitance C_2 results after 1500 hardening days are depicted in Figure 7. The highest value of this parameter was noted for the GP20 specimens, followed by the GP10 ones. On the other hand, the reference samples showed the lowest capacitance C_2 in over the very long term.

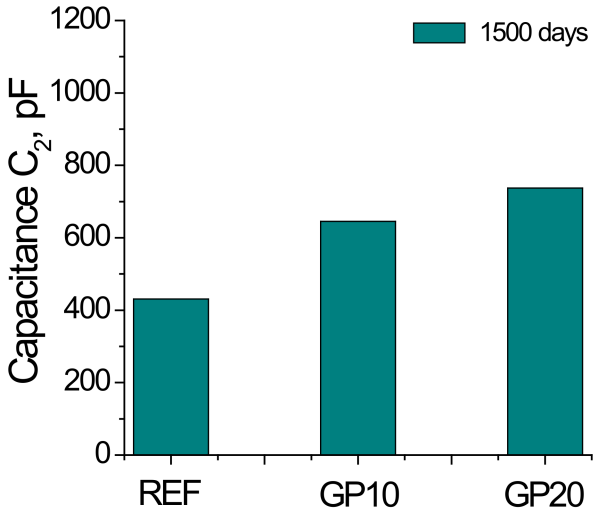

Figure 7. Values of capacitance C_2 noted for the REF, GP10, and GP20 specimens.

In relation to impedance resistance R_2, the results can be observed in Figure 8. This resistance was considerably greater for the glass powder samples after 1500 hardening days compared with reference ones. Furthermore, the value of this parameter rose along with the higher percentage of glass powder addition in the mortar, with the highest resistance R_2 noted for the GP20 specimens.

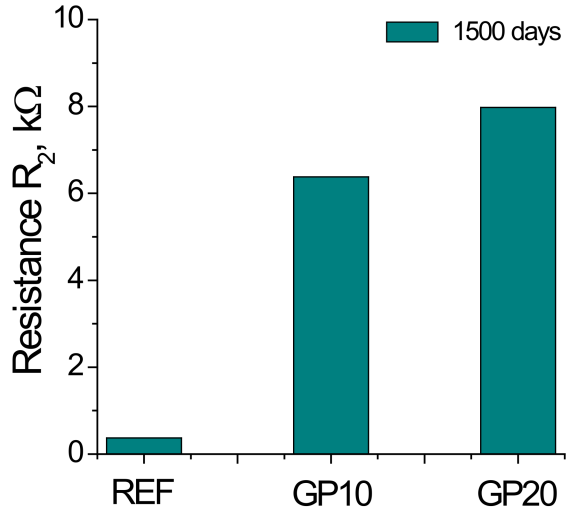

Figure 8. Results of capacitance R_2 obtained for the different mortar series tested.

3.3. Differential Thermal Analysis

The derivate of the weight versus temperature curves obtained for the analyzed mortar series after 1500 hardening ages are depicted in Figure 9. The area of portlandite peak of this curve lowered as the percentage of clinker replacement by waste glass powder increased.

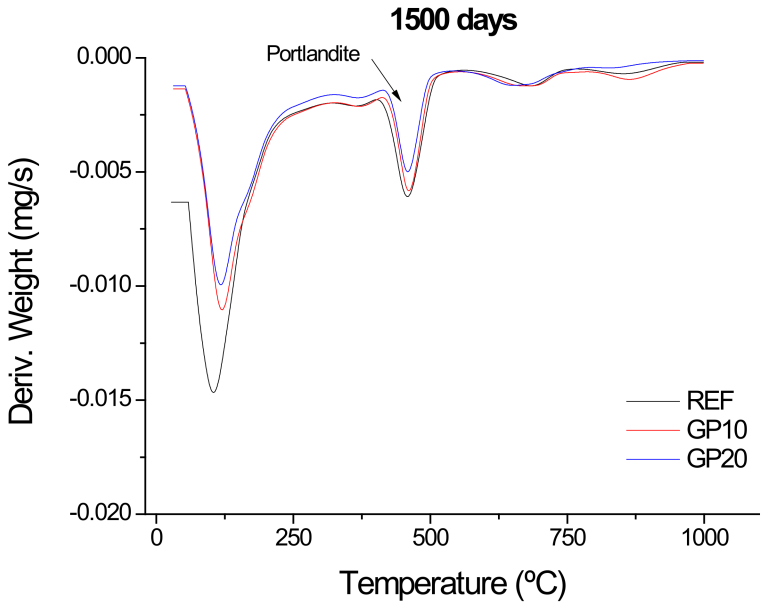

Figure 9. Derivate of weight versus temperature curve obtained for the studied mortars after 1500 hardening days.

3.4. X-Ray Diffraction (XRD)

The X-ray spectra obtained for each mortar series studied after 1500 hardening days are depicted in Figure 10. As can be observed, the analysis of the peak intensities showed a portlandite decrease as the percentage of clinker replacement by waste glass powder increased in the sample.

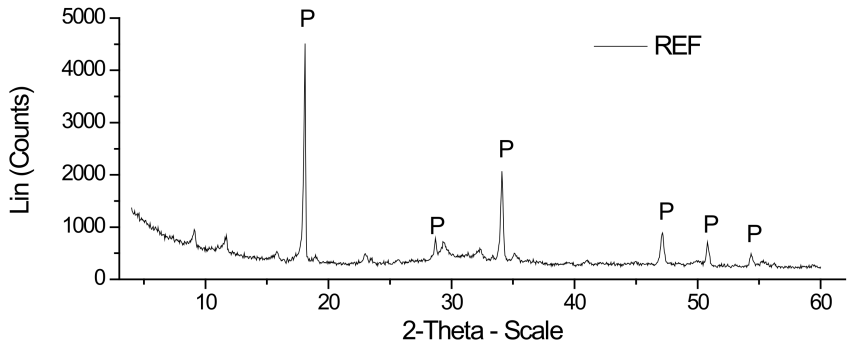

(**a**)

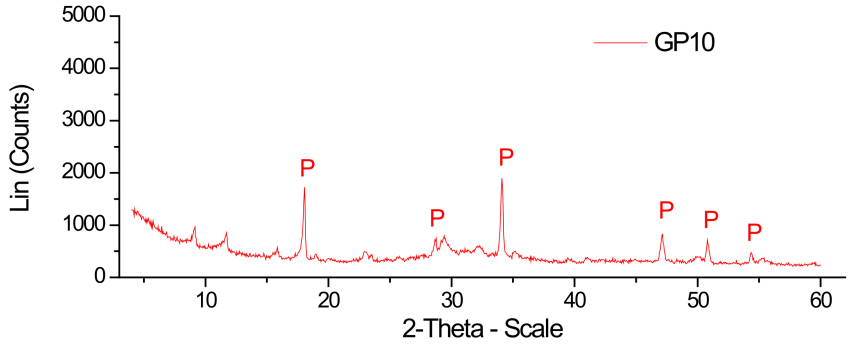

(**b**)

Figure 10. *Cont.*

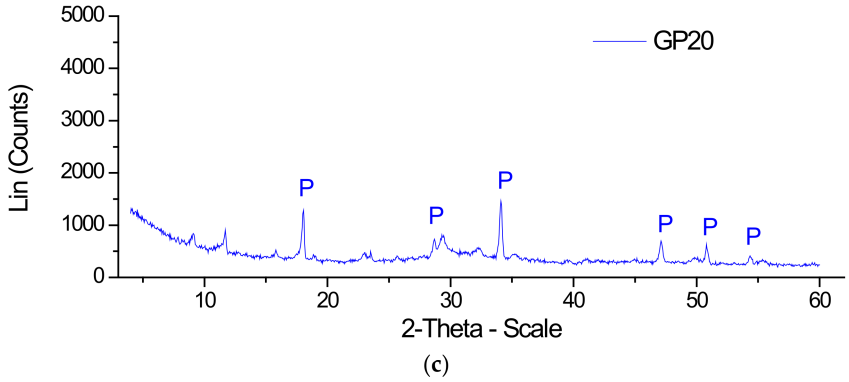

Figure 10. (**a**) XRD spectrum for REF mortars; (**b**) XRD spectrum for GP10 mortars; (**c**) XRD spectrum for GP20 mortars. The letter P indicates the portlandite peaks in each spectrum.

3.5. Water Absorption

The results of the percentages of water absorption after immersion determined according to ASTM Standard C642-06 [39] can be observed in Figure 11. This parameter was very similar for all of the mortar series analyzed after 1500 hardening days. It was slightly higher for GP20 and slightly lower for GP10, when comparing both with the REF specimens, although in both cases the differences between them were not noticeable.

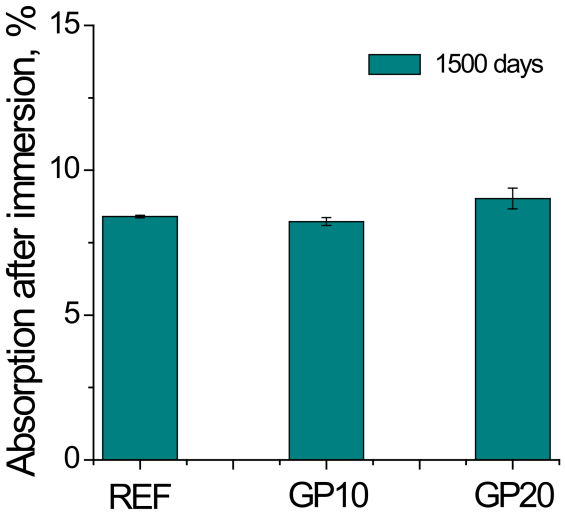

Figure 11. Percentages of absorption after immersion determined according to ASTM Standard C642-06 [39] for the REF, GP10, and GP20 mortars.

3.6. Steady-State Chloride Diffusion Coefficient

The results of the steady-state chloride diffusion coefficient obtained from sample's resistivity for the studied mortars in the very long term are represented in Figure 12. The greatest value of this coefficient was observed for the reference specimens. Mortars with glass powder showed lower steady-state diffusion coefficients compared with the reference ones. Finally, it is interesting to highlight that the lowest value for this parameter was noted for the specimens with the higher waste glass content (GP20 series).

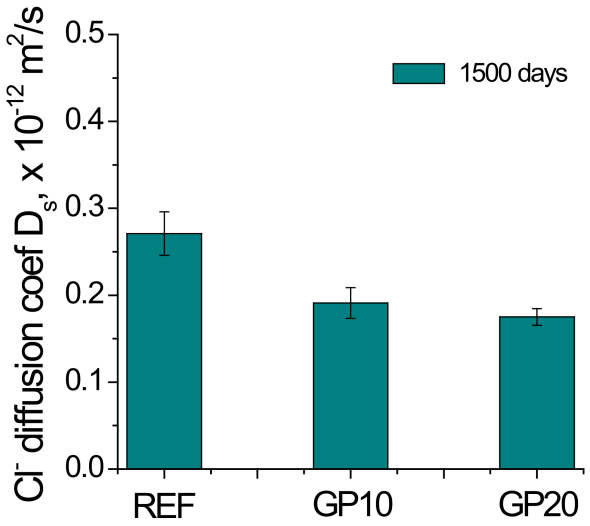

Figure 12. Results of the steady-state chloride diffusion coefficient obtained from the samples' resistivity for the studied mortars after1500 hardening days.

3.7. Length Change

The percentage of length change with respect to the initial length noted for the mortar series studied after 1500 hardening days is represented in Figure 13. As can be observed, all of the mortars experienced an expansion during the analyzed time period. This expansion was higher for the REF samples. In relation to the mortars with glass powder, this expansion was slightly lower for the GP20 mortars, although in general it was relatively similar for both GP series.

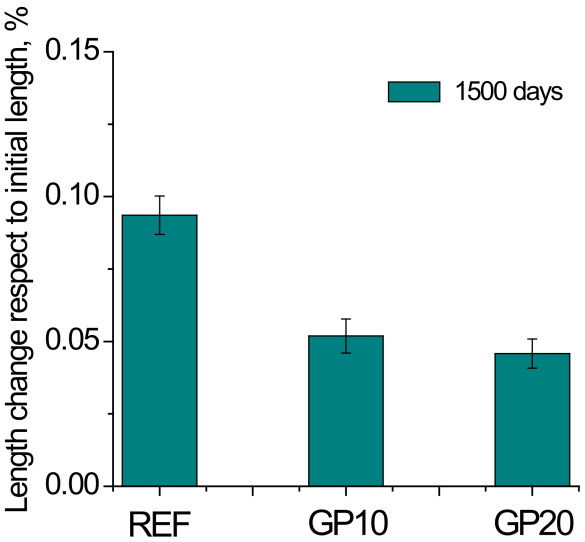

Figure 13. Percentage of length change respect to the initial length noted for REF, GP10 and GP20 mortars after 1500 hardening days.

4. Discussion

Regarding the microstructure characterization, the results of the mercury intrusion porosimetry and impedance spectroscopy technique showed coincidences. On one hand, in relation to the solid fraction of the mortars, both techniques showed that it was very similar for all of the mortars studied after 1500 hardening days. In particular, the impedance capacitance C_1 provided information about the global solid fraction in the sample [36], independently of its pore size distribution, while the total porosity gave data about the global volume of pores. Therefore, the similar values for both of the parameters noted

for all the mortars (see Figures 3 and 6) would suggest that there were scarce differences in their global solid fraction and pores volume, independently of the addition of waste glass powder, at least for the percentages of clinker replacement studied here. This minor influence in the global porosity has been observed for other classical additions, such as fly ash [42].

With respect to the pore size distributions of the mortars, the mercury intrusion porosimetry technique (see Figure 4) showed that specimens with waste glass powder had a more refined microstructure, with a higher percentage of pores with smaller diameters, especially for those with sizes lower than 10 nm. In addition, it has also been noted that the higher content of glass powder in the binder produced a greater pore refinement. The percentage of Hg retained at the end of porosimetry test (see Figure 5) was slightly higher for the GP mortars, which would also suggest a greater tortuosity of the pore network in these specimens.

The results of the impedance capacitance C_2 (see Figure 7) and resistance R_2 (see Figure 8) were in keeping with the pore size distributions obtained with mercury intrusion porosimetry. The capacitance C_2 is associated with the pore surface in contact with the electrolyte that fills the pore network of the material [37], while the R_2 resistance provides information about the pores [37]. The capacitance C_2 increased along with the increased percentage of waste glass powder in the binder, which would suggest that mortars with this addition had a greater pore surface [30,43]. Regarding impedance resistance R_2, the greater values of this parameter noted for the GP10 and GP20 specimens would indicate that their pore structure would have the presence of more fine pores, coinciding with the information provided by the pore size distributions.

The pore refinement produced by the glass powder in the very long term would be as a result of the development of the pozzolanic reactions of this addition [15,27,28]. These pozzolanic reactions would produce a solid phase formation, closing the microstructure, reducing the size of the pores, and increasing their surface, because of the appeareance of the new solid structures on the preexisting pore walls. This pozzolanic activity of the waste glass powder after 1500 hardening days was confirmed by the results of differential thermal analysis, which showed a lower area of portlandite peak in the curves derivate of weight versus temperature for the GP mortars compared with reference ones (see Figure 9). In addition, the lower intensities of portlandite peaks for the series with glass powder revealed by the analyses of XRD spectra would also indicate this pozzolanic activity in the very long term for this addition. These results are in agreement with those observed by other authors [20,30,44] for shorter hardening ages.

In relation to durability-related properties, the percentage of absorption after immersion was relatively similar for all of the mortars studied (see Figure 11), being in accordance with total porosity and capacitance C_1 results, which would show hardly any differences in the overall solid fraction and volume of pores between the different analyzed binders. With regard to the steady-state chloride diffusion coefficient, it is important to get the information for the very long term, because chlorides are one of the most harmful agents that could produce the corrosion of reinforcements embedded in cement-based materials. As has been previously described, the values of this coefficient were noticeably lower for mortars with glass powder (see Figure 12). This result could be related to the higher pore refinement observed for the GP10 and GP20 specimens, compared with the REF ones, which would be produced by the development of pozzolanic reactions of glass powder [28], as already discussed. The greater presence of finer pores would make the movement of chlorides through the microstructure of mortars more difficult, entailing lower diffusion coefficients, as has been noted.

Regarding the results of the length change noted for the different mortars series studied (see Figure 13), a length increase for all of them was observed, which would indicate that an expansion was produced. This result would be expected, because the mortars were stored under optimum laboratory conditions until the testing age at 1500

hardening days. Nevertheless, it is important to highlight that the GP mortars showed less expansion compared with the reference ones.

According to the results previously discussed, it seems that the addition of waste glass powder in mortars, up to 20% of the clinker replacement, would have beneficial effects after 1500 hardening days, in terms of microstructure refinement and resistance against chloride ingress, without worsening other parameters such as the total porosity and water absorption through immersion. In the very long term, these results would be relevant in order to assess the future use for real construction elements of waste glass powder addition, because the required service life of these elements belonging to buildings and other engineering works are usually long.

Finally, it has been reported greenhouse gasses analyses [45] that showed that a substitution of 10% of clinker by waste glass powder would make a reduction of approximately 9% of CO_2 emissions per ton of cement produced [45], compared with cement type I without additions. For a percentage of replacement of 20% of clinker by waste glass powder, around an 18% reduction of CO_2 emissions per ton of cement produced has been estimated [45]. Therefore, in addition to the beneficial effects in the microstructure and chloride diffusion in the very long term, the incorporation of glass powder in binders for cement-based materials would also contribute to sustainability, with added value from an environmental point of view.

5. Conclusions

The main conclusions that can be drawn from the results previously discussed can be summarized as follows:

- After 1500 hardening days, the microstructure of mortars that incorporated waste glass powder was more refined compared with the reference specimens, according to the pore size distributions, obtained with mercury intrusion porosimetry, and the impedance spectroscopy parameters capacitance C_2 and resistance R_2. The microstructure became more refined as the percentage of waste glass powder in the mortars increased.
- The higher pore refinement produced by waste glass powder could be due to the pozzolanic activity of this addition, as suggested the differential thermal analyses after 1500 hardening days, resulting in a higher presence of finer pores.
- The global solid fraction and pore volumes of the mortars was very similar after 4 years, independently of the incorporation of waste glass powder in the binder, as suggested by the total porosity results, determined with mercury intrusion porosimetry, as well as the impedance spectroscopy capacitance C_1.
- The addition of waste glass powder did not worsen the behaviour of the mortars over the very long term in relation to the water absorption after immersion.
- Mortars with glass powder showed lower steady-state chloride diffusion coefficients after 1500 days in comparison with the reference specimens. Furthermore, this coefficient lowered as the proportion of glass powder in the binder increased. This good performance related to the chloride diffusion could be as a result of the more refined pore structure produced by the waste glass powder addition.
- In view of the results observed in this research, the incorporation of 10% and 20% of waste glass powder as a substitution for the clinker would produce an adequate behaviour in mortars after approximately 4 hardening years, improving their microstructure and chloride ingress resistance, without affecting their water absorption.

Author Contributions: Conceptualization, V.L. and J.M.O.; methodology, V.L., T.R.-H. and J.M.O.; investigation, R.M.T., T.R.-H. and J.M.O.; data curation, R.M.T., F.G.B. and J.M.O.; writing—original draft preparation, R.M.T.; writing—review and editing, J.M.O., V.L. and F.G.B.; supervision, T.R.-H. and J.M.O.; funding acquisition, J.M.O., V.L. and F.G.B. The results included in this paper were obtained in the Ph.D. thesis carried out by R.M.T. at University of Alicante (Spain), under the supervision of J.M.O. and T.R.-H. All authors have read and agreed to the published version of the manuscript.

Funding: This work was supported by the Conselleria de Educación, Investigación, Cultura y Deporte (presently re-named as Conselleria de Innovación, Universidades, Ciencia y Sociedad Digital) de la Generalitat Valenciana, Spain (grant code GV/2019/070); by the Agencia Nacional de Investigación y Desarrollo de Chile (ANID; grant number FONDECYT REGULAR 1211135); by FCT-Foundation for Science and Technology, IP, within the scope of the R&D Unit Institute for sustainability and innovation in structural engineering-ISISE (UIDP/04029/2020); and by the ERDF through the COMPETE 2020 program, Portugal 2020 (project POCI-01-0247-FEDER-033990 iNBRail).

Institutional Review Board Statement: Not applicable.

Informed Consent Statement: Not applicable.

Data Availability Statement: Not applicable.

Acknowledgments: The authors wish to thank Cementos Portland Valderrivas S.A. for providing the ordinary Portland cement used in this study.

Conflicts of Interest: The authors declare no conflict of interest.

References

1. Benhelal, E.; Shamsaei, E.; Rashid, M.I. Challenges against CO_2abatement strategies in cement industry: A review. *J. Environ. Sci.* **2021**, *104*, 84–101. [CrossRef]
2. Zhang, C.-Y.; Yu, B.; Chen, J.-M.; Wei, Y.-M. Green transition pathways for cement industry in China. *Resour. Conserv. Recycl.* **2021**, *166*. [CrossRef]
3. Rodríguez, G.; Medina, C.; Alegre, F.J.; Asensio, E.; Sánchez de Rojas, M.I. Assessment of Construction and Demolition Waste plant management in Spain: In pursuit of sustainability and eco-efficiency. *J. Clean. Prod.* **2015**, *90*, 16–24. [CrossRef]
4. Valipour, M.; Shekarchi, M.; Arezoumandi, M. Chlorine diffusion resistivity of sustainable green concrete in harsh marine environments. *J. Clean. Prod.* **2017**, *142*, 4092–4100. [CrossRef]
5. Yang, K.-H.; Jung, Y.-B.; Cho, M.-S.; Tae, S.-H. Effect of supplementary cementitious materials on reduction of CO2 emissions from concrete. *J. Clean. Prod.* **2015**, *103*, 774–783. [CrossRef]
6. Mirza, J.; Mirza, M.; Roy, V.; Saleh, K. Basic rheological and mechanical properties of high-volume fly ash grouts. *Constr. Build. Mater.* **2002**, *16*, 353–363. [CrossRef]
7. Thomas, M.D.A.; Scott, A.; Bremner, T.; Bilodeau, A.; Day, D. Performance of slag concrete in marine environment. *ACI Mater. J.* **2008**, *105*, 628–634.
8. Xu, W.; Lo, Y.T.; Wang, W.; Ouyang, D.; Wang, P.; Xing, F. Pozzolanic Reactivity of Silica Fume and Ground Rice Husk Ash as Reactive Silica in a Cementitious System: A Comparative Study. *Materials* **2016**, *9*, 146. [CrossRef]
9. Navrátilová, E.; Rovnaníková, P. Pozzolanic properties of brick powders and their effect on the properties of modified lime mortars. *Constr. Build. Mater.* **2016**, *120*, 530–539. [CrossRef]
10. Ribeiro, D.V.; Labrincha, J.A.; Morelli, M.R. Potential use of natural red mud as pozzolan for Portland cement. *Mater. Res.* **2011**, *14*, 60–66. [CrossRef]
11. Rashad, A.M. Recycled waste glass as fine aggregate replacement in cementitious materials based on Portland cement. *Constr. Build. Mater.* **2014**, *72*, 340–357. [CrossRef]
12. EPA Advancing Sustainable Materials Management: Facts and Figures. Available online: https://www.epa.gov/smm/advancing-sustainable-materials-management-facts-and-figures (accessed on 20 January 2020).
13. FEVE Best Performing Bottle to Bottle Closed Loop Recycling System. Available online: http://feve.org/wp-content/uploads/2016/04/Press-Release-EU.pdf (accessed on 20 January 2020).
14. Aliabdo, A.A.; Abd Elmoaty, A.E.M.; Aboshama, A.Y. Utilization of waste glass powder in the production of cement and concrete. *Constr. Build. Mater.* **2016**, *124*, 866–877. [CrossRef]
15. Matos, A.M.; Sousa-Coutinho, J. Durability of mortar using waste glass powder as cement replacement. *Constr. Build. Mater.* **2012**, *36*, 205–215. [CrossRef]
16. Shao, Y.; Lefort, T.; Moras, S.; Rodriguez, D. Studies on concrete containing ground waste glass. *Cem. Concr. Res.* **2000**, *30*, 91–100. [CrossRef]
17. Schwarz, N.; Neithalath, N. Influence of a fine glass powder on cement hydration: Comparison to fly ash and modeling the degree of hydration. *Cem. Concr. Res.* **2008**, *38*, 429–436. [CrossRef]
18. Shayan, A.; Xu, A. Value-added utilisation of waste glass in concrete. *Cem. Concr. Res.* **2004**, *34*, 81–89. [CrossRef]
19. Parghi, A.; Shahria Alam, M. Physical and mechanical properties of cementitious composites containing recycled glass powder (RGP) and styrene butadiene rubber (SBR). *Constr. Build. Mater.* **2016**, *104*, 34–43. [CrossRef]
20. Kamali, M.; Ghahremaninezhad, A. Effect of glass powders on the mechanical and durability properties of cementitious materials. *Constr. Build. Mater.* **2015**, *98*, 407–416. [CrossRef]
21. Shayan, A.; Xu, A. Performance of glass powder as a pozzolanic material in concrete: A field trial on concrete slabs. *Cem. Concr. Res.* **2006**, *36*, 457–468. [CrossRef]

22. Du, H.; Tan, K.H. Properties of high volume glass powder concrete. *Cem. Concr. Compos.* **2017**, *75*, 22–29. [CrossRef]
23. Serpa, D.; Santos Silva, A.; De Brito, J.; Pontes, J.; Soares, D. ASR of mortars containing glass. *Constr. Build. Mater.* **2013**, *47*, 489–495. [CrossRef]
24. Madandoust, R.; Ghavidel, R. Mechanical properties of concrete containing waste glass powder and rice husk ash. *Biosyst. Eng.* **2013**, *116*, 113–119. [CrossRef]
25. Ling, T.-C.; Poon, C.-S.; Kou, S.-C. Feasibility of using recycled glass in architectural cement mortars. *Cem. Concr. Compos.* **2011**, *33*, 848–854. [CrossRef]
26. Omran, A.; Tagnit-Hamou, A. Performance of glass-powder concrete in field applications. *Constr. Build. Mater.* **2016**, *109*, 84–95. [CrossRef]
27. Letelier, V.; Tarela, E.; Osses, R.; Cárdenas, J.P.; Moriconi, G. Mechanical properties of concrete with recycled aggregates and waste glass. *Struct. Concr.* **2017**, *18*, 40–53. [CrossRef]
28. Kamali, M.; Ghahremaninezhad, A. An investigation into the hydration and microstructure of cement pastes modified with glass powders. *Constr. Build. Mater.* **2016**, *112*, 915–924. [CrossRef]
29. Bignozzi, M.C.; Saccani, A.; Barbieri, L.; Lancellotti, I. Glass waste as supplementary cementing materials: The effects of glass chemical composition. *Cem. Concr. Compos.* **2015**, *55*, 45–52. [CrossRef]
30. Khmiri, A.; Chaabouni, M.; Samet, B. Chemical behaviour of ground waste glass when used as partial cement replacement in mortars. *Constr. Build. Mater.* **2013**, *44*, 74–80. [CrossRef]
31. European Committee for Standardization. *EN 1992-1-1 Eurocode 2: Design of Concrete Structures—Part 1-1: General Rules and Rules for Buildings*; CEN: Brussels, Belgium, 2004.
32. AENOR UNE-EN 197-1:2011. *Composición, Especificaciones y Criterios de Conformidad de los Cementos Comunes*; Asociación Española de Normalización y Certificación: Madrid, Spain, 2011; p. 30.
33. AENOR UNE-EN 196-1:2005. *Métodos de Ensayo de Cementos. Parte 1: Determinación de Resistencias Mecánicas*; Asociación Española de Normalización y Certificación: Madrid, Spain, 2005.
34. Diamond, S. Mercury porosimetry. *Cem. Concr. Res.* **2000**, *30*, 1517–1525. [CrossRef]
35. Ouellet, S.; Bussière, B.; Aubertin, M.; Benzaazoua, M. Microstructural evolution of cemented paste backfill: Mercury intrusion porosimetry test results. *Cem. Concr. Res.* **2007**, *37*, 1654–1665. [CrossRef]
36. Cabeza, M.; Merino, P.; Miranda, A.; Nóvoa, X.R.; Sanchez, I. Impedance spectroscopy study of hardened Portland cement paste. *Cem. Concr. Res.* **2002**, *32*, 881–891. [CrossRef]
37. Cabeza, M.; Keddam, M.; Nóvoa, X.R.; Sánchez, I.; Takenouti, H. Impedance spectroscopy to characterize the pore structure during the hardening process of Portland cement paste. *Electrochim. Acta* **2006**, *51*, 1831–1841. [CrossRef]
38. Tang, S.W.; Cai, X.H.; He, Z.; Zhou, W.; Shao, H.Y.; Li, Z.J.; Wu, T.; Chen, E. The review of pore structure evaluation in cementitious materials by electrical methods. *Constr. Build. Mater.* **2016**, *117*, 273–284. [CrossRef]
39. ASTM. *ASTM C642—06 Standard Test Method for Density, Absorption, and Voids in Hardened Concrete*; ASTM International: West Conshohocken, PA, USA, 2006; p. 3.
40. Andrade, C.; Alonso, C.; Arteaga, A.; Tanner, P. Methodology based on the electrical resistivity for the calculation of reinforcement service life. In Proceedings of the 5th CANMET/ACI International Conference on Durability of Concrete, Supplementary Papers, Barcelona, Spain, 4–9 June 2000; Malhotra, V.M., Ed.; American Concrete Institute: Farmington Hills, MI, USA, 2000; pp. 899–915.
41. ASTM. *ASTM C596—01 Standard Test Method for Drying Shrinkage of Mortar Containing Hydraulic Cement*; ASTM International: West Conshohocken, PA, USA, 2001; p. 3.
42. Bijen, J. Benefits of slag and fly ash. *Constr. Build. Mater.* **1996**, *10*, 309–314. [CrossRef]
43. Kim, J.; Yi, C.; Zi, G. Waste glass sludge as a partial cement replacement in mortar. *Constr. Build. Mater.* **2015**, *75*, 242–246. [CrossRef]
44. Lu, J.-X.; Zhan, B.-J.; Duan, Z.-H.; Poon, C.S. Improving the performance of architectural mortar containing 100% recycled glass aggregates by using SCMs. *Constr. Build. Mater.* **2017**, *153*, 975–985. [CrossRef]
45. Letelier, V.; Henríquez-Jara, B.I.; Manosalva, M.; Parodi, C.; Ortega, J.M. Use of waste glass as a replacement for raw materials in mortars with a lower environmental impact. *Energies* **2019**, *12*, 1974. [CrossRef]